

Probing protein-peptide binding surfaces using charged stable free radicals and transverse paramagnetic relaxation enhancement (PRE)

Michaël L. Deschamps*, Ewa S. Pilka, Jennifer R. Potts, Iain D. Campbell & Jonathan Boyd

Department of Biochemistry, University of Oxford, South Parks Road, OX1 3QU Oxford, U.K.

Received 25 October 2004; Accepted 6 December 2004

Key words: complex, nitroxide, NMR, spin-label, TEMPO

Abstract

Nitroxide species, which have an unpaired electron localized on a nitrogen atom, can be useful as NMR probes to identify areas of the surface of a protein involved in the formation of a complex. The proximity of an electron spin leads to higher NMR relaxation rates for protein nuclei. If a protein–ligand complex is formed the radical is excluded from certain sites on the protein surface, protecting them from relaxation effects. We show here that charged nitroxide species can be helpful for identifying regions of the surface of the ⁴F1⁵F1 module pair from human fibronectin involved in peptide binding.

Solutions containing paramagnetic solutes influence nuclear relaxation via the strong local magnetic fields produced by the magnetic moment of the unpaired electron(s). This feature has often been applied to probe specific details of protein structure and dynamics (Dwek, 1973; Ball et al., 1999; Hustedt and Beth, 1999; Barnakov et al., 2002; Brown et al., 2002; Gross and Hubbell, 2002; Ulmer et al., 2002; Bhargava and Feix, 2004). In the absence of either covalent attachment or a specific strong binding site, protein-radical interactions in solution can, in general, be assumed to exhibit very short random lifetimes, which vary for different protein sites; these interactions are governed primarily by diffusion processes. The quadratic dependence of paramagnetic relaxation enhancement on the magnetogyric ratio, γ_1 , of the nuclear spin makes the ¹H nucleus particularly sensitive to effects from paramagnetic substances such as nitroxide and trityl radicals or even from dissolved oxygen (Teng and Bryant, 2000; Prosser et al., 2001; Ulmer et al., 2002). For a diffusion

model of dipole–dipole electron–nuclear interactions, an important influence upon nuclear relaxation is expected from the translational diffusion correlation time, τ_d , governed by the relative translational self-diffusion coefficients of the protein, D_p , and the free radical, D_{fr} , the distance of closest approach, d , between a ¹H nucleus and a radical and the local radical concentration surrounding the ¹H nucleus. Assigning the values $D_p \approx 5 \times 10^{-11} \text{ m}^2 \text{ s}^{-1}$, $D_{fr} \approx 40 \times 10^{-11} \text{ m}^2 \text{ s}^{-1}$ and $d \approx 5 \text{ \AA}$, which are typical values for the types of systems under discussion here, an approximate estimate for τ_d can be obtained from the relationship $\tau_d = 2d^2 / (D_p + D_{fr})$ giving a value for τ_d of $\sim 1.1 \text{ ns}$. The dipolar interaction will also be influenced by the electron spin longitudinal relaxation time, T_{1e} , when this is faster than the translational diffusion correlation time ($T_{1e} < \tau_d$), i.e. if the electron spin changes its orientation before the protein-radical orientation changes. However, for nitroxide and trityl radicals T_{1e} is typically found to be in the region of $\sim 10\text{--}500 \text{ \mu s}$ (Hass et al., 1993) and assuming the effective correlation time, τ , for the fluctuation of the electron–nuclear dipolar interaction

*To whom correspondence should be addressed. E-mail: Michael.Deschamps@bioch.ox.ac.uk

can be written as $\tau^{-1} = T_{1e}^{-1} + \tau_d^{-1}$ is expected to be dominated by the diffusion process.

The use of the nitroxide radical TEMPOL as a molecular probe is well established (Niccolai et al., 1984; Esposito et al., 1992; Molinari et al., 1997; Scarselli et al., 1999). Typically for these studies the TEMPOL radical has been used at relatively high concentrations (50 mM) and the radical accessible protein surface is characterized by the disappearance of resonances from the spectrum due to paramagnetic relaxation enhancement (PRE) although the use of such high concentrations can lead to a general broadening of resonances.

The present study investigates the use of low concentrations of charged nitroxide radicals, in addition to non-charged TEMPOL, as an aid for identifying regions of a protein surface involved in ligand binding. For those residues on the protein surface involved in binding interactions, the ligand provides protection from any non-specific weak protein radical interactions, thus leading to changed PRE effects between the free and complexed forms of the protein. The residue specific differential PRE effects, $\Delta(\text{PRE})$, due to the protein-ligand binding interaction provides a complementary dataset to a chemical shift map of the same system (Pellechia et al., 2002).

The $^4\text{F}1^5\text{F}1$ module pair (residues 152–244) of mature human fibronectin binds to the C-terminal region of the fibronectin binding protein FnBPA from *Staphylococcus aureus*. The peptide fragment D3t (cKPSYQFGGHNSVDFEEDTLPKVn) in FnBPA contains correctly ordered F1 binding motifs for binding to the sequential modules $^4\text{F}1^5\text{F}1$, $K_D = 8.1 \pm 0.6 \mu\text{M}$ (Schwarz-Linek et al., 2003). The site-specific $^1\text{H}^{\text{N}}$ transverse PRE from the $^4\text{F}1^5\text{F}1$ module pair was measured, both free and complexed to the D3t peptide, using the nitroxide radicals shown in Figure 1.

The $^4\text{F}1^5\text{F}1$ protein was expressed as described elsewhere (Penkett et al., 2000) and all NMR measurements were performed at temperature $T = 37^\circ\text{C}$ on a spectrometer operating at 500 MHz for ^1H and the pH of the samples was adjusted to five. The D3t peptide was purchased from Alta Bioscience, Birmingham, U.K. and used after purification by HPLC. Dioxan, TEMPOL, 3-carboxy-PROXYL and 4-amino-TEMPO were purchased from Sigma and used without further purification. Solutions of 3-carboxy-PROXYL were obtained by adding small amounts of 1 M

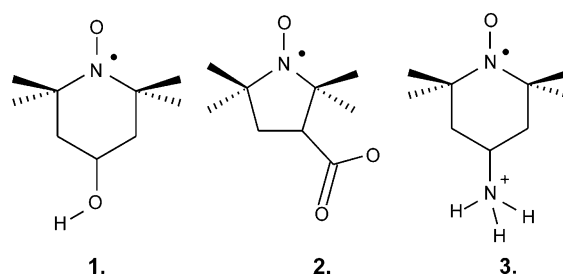


Figure 1. Neutral and charged nitroxide moieties for probing the peptide binding surface in the $^4\text{F}1^5\text{F}1$ module pair: (1) TEMPOL: 4-hydroxy-2,2,6,6-tetramethyl-1-piperidinyloxy (2) 3-carboxy-PROXYL: 3-carboxy-2,2,5,5-tetramethyl-1-pyrrolidinyloxy (3) 4-amino-TEMPO: 4-amino-2,2,6,6-tetramethyl-1-piperidinyloxy. Each molecule is soluble in aqueous solution in the range pH 5–8 and over this range of pH is associated with a charge of 0, $-e$, and $+e$ respectively. For illustrative purposes only the unpaired electron is shown as being completely localized on the N atom.

NaOH. The $^1\text{H}^{\text{N}}$ and ^{15}N transverse relaxation rates were measured using a CPMG (Carr and Purcell, 1954; Meiboom and Gill, 1958) sequence for dioxan and a two dimensional CPMG-HSQC (Carr and Purcell, 1954; Meiboom and Gill, 1958, Bodenhausen and Rubex, 1980) sequence for the backbone $^4\text{F}1^5\text{F}1$ $^1\text{H}^{\text{N}}$ nuclei.

In order to gain insight into the dependence of the ^1H transverse PRE upon concentration of each nitroxide species, the transverse relaxation rate (R_2) of the dioxan ^1H nucleus (0.8 mM) in solutions containing varying radical concentrations (0–10 mM) was measured using a CPMG sequence (Carr et al., 1954). The concentration dependence of the transverse PRE was measured by monitoring the change to the dioxan ^1H transverse relaxation rate, $\Delta R_2(\text{PRE}) = R_{2(\text{dioxan} + \text{nitroxide})} - R_{2(\text{dioxan})}$. To a good approximation, for this simple system, the dioxan transverse relaxation rate was found to depend linearly upon radical concentration in the range from 0 to 10 mM. The proportionality coefficients $\Delta R_2(\text{PRE})/[\text{Radical}/\text{M}]$ for the 3-carboxy-PROXYL, 4-amino-TEMPO and TEMPOL species are similar (173 ± 2 , 102 ± 0.3 and $182 \pm 15 \text{ s}^{-1}\text{mol}^{-1}$ respectively) with the 4-amino TEMPO species being slightly less effective.

For the backbone $^1\text{H}^{\text{N}}$ of the non-complexed $^4\text{F}1^5\text{F}1$ module pair, the transverse PRE effect from each nitroxide radical, $\Delta R_2(\text{PRE})_{\text{free}}$, was measured as the difference in $^1\text{H}^{\text{N}}$ transverse relaxation rate between two datasets recorded

with $((R_2)_{\text{free}} + \Delta R_2(\text{PRE})_{\text{free}})$ and without radical $((R_2)_{\text{free}})$. These data are shown in Figure 2a. For two residues (43 and 88) no detectable signal could be observed using the 3-carboxy-PROXYL species, even at relatively low concentrations (5 mM) of radical. Although a PRE value could not be measured directly for residues 43 and 88, the PRE effect is estimated to make a contribution to the transverse relaxation rate of at least ~ 230 Hz and ~ 260 Hz respectively. In the absence of radical, for a given peak in an 2D-HSQC experiment, the signal intensity to noise ratio, S/N_0 , is proportional to $\exp(-\tau_{\text{exp}}R_2)/R_2$, where τ_{exp} is the effective duration of the pulse sequence (for a standard HSQC, $\tau_{\text{exp}} \approx 11$ ms), during which the $^1\text{H}^{\text{N}}$ magnetization is affected by transverse relaxation. If nitroxide radical is added, a PRE effect ($\Delta R_2(\text{PRE})$) can be measured and the new signal intensity to noise ratio S/N_1 is proportional to $\exp(-\tau_{\text{exp}}[R_2 + \Delta R_2(\text{PRE})])/[R_2 + \Delta R_2(\text{PRE})]$. No significant differences to the longitudinal (T_1) paramagnetic relaxation enhancement was detected for any of the $^1\text{H}^{\text{N}}$ nuclei in $^4\text{F1}^5\text{F1}$ when using nitroxide concentrations below 10 mM. Within the assumption that $R_2(^1\text{H}^{\text{N}})$ is constant between the experiments performed with and without radical the signal intensity to noise ratios are related via Equation 1:

$$\frac{(S/N_0)/(S/N_1)}{\exp(t_{\text{exp}}\Delta R_2(\text{PRE}))} = [1 + \Delta R_2(\text{PRE})/R_2] \quad (1)$$

allowing a lower limit for $\Delta R_2(\text{PRE})$ to be estimated assuming $S/N_1 = 1$ and the experimental value for S/N_0 . For the free $^4\text{F1}^5\text{F1}$ species a combined total of 10 $^1\text{H}^{\text{N}}$ nuclei for the three radicals were found to exhibit a minimum $\Delta R_2(\text{PRE})_{\text{free}}$ effect > 25 Hz (14, 24, 25, 35, 41, 43, 44, 67, 88 and 90).

A similar series of PRE datasets, $\Delta R_2(\text{PRE})_{\text{bound}}$, were measured for $^4\text{F1}^5\text{F1}$ fully complexed to the D3t peptide in the presence of similar concentrations of each radical and these data are shown in Figure 2b. The PRE variation between the complexed and free species, ($\Delta\text{PRE} = \Delta R_2(\text{PRE})_{\text{bound}} - \Delta R_2(\text{PRE})_{\text{free}}$), as a function of residue number for each radical is shown in Figure 2c. These data show the $^1\text{H}^{\text{N}}$ nuclei exhibiting a significantly differential PRE effect – ΔPRE – upon complex formation and 13 $^1\text{H}^{\text{N}}$ nuclei exhibit a minimum ΔPRE of at least

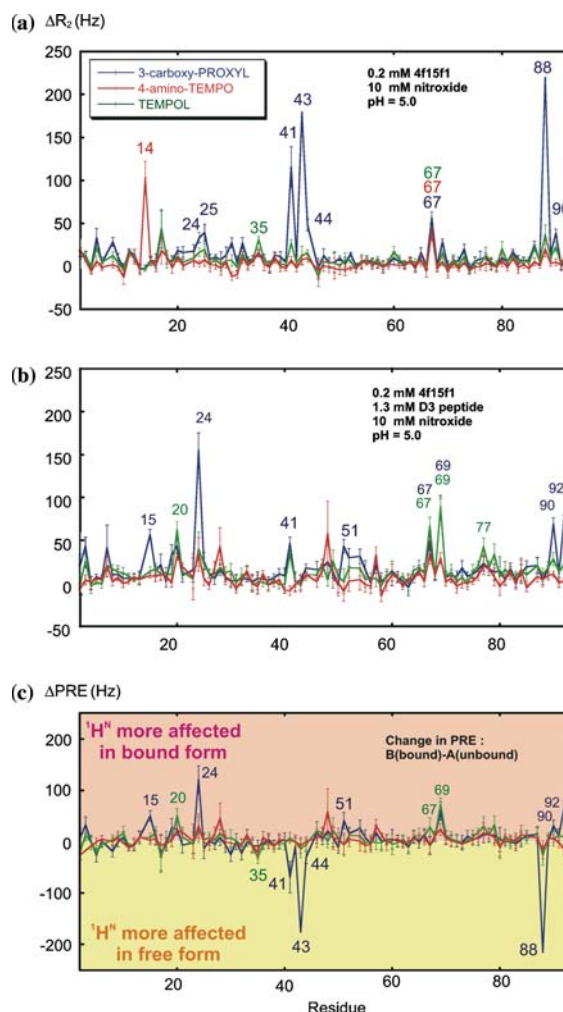


Figure 2. (a) $^1\text{H}^{\text{N}}$ transverse PRE as a function of residue number recorded from solutions of ^{15}N isotopically enriched $^4\text{F1}^5\text{F1}$, pH 5, containing 10 mM of either 3-carboxy-PROXYL (blue), 4-amino-TEMPO (red) or TEMPOL (green). (b) $^1\text{H}^{\text{N}}$ transverse PRE as a function of residue number recorded from solutions of ^{15}N isotopically enriched $^4\text{F1}^5\text{F1}$ containing a small molar excess of the D3t peptide, pH 5, and 10 mM of either 3-carboxy-PROXYL (blue), 4-amino-TEMPO (red) or TEMPOL (green). The residue numbers of those $^1\text{H}^{\text{N}}$ nuclei exhibiting the largest transverse PRE are highlighted. (c) The change in $\Delta R_2(\text{PRE}) - \Delta\text{PRE}$ – highlights the $^1\text{H}^{\text{N}}$ relaxation rates most affected by the binding of the ligand. The $^1\text{H}^{\text{N}}$ line width was determined from a series of ^{15}N - ^1H 2-Dimensional CPMG-HSQC datasets, i.e., a train of spin echoes applied on protons followed by a HSQC filter to select the $^1\text{H}^{\text{N}}$ - ^{15}N pairs (Carr and Purcell, 1954; Meiboom and Gill, 1958; Bodenhausen and Rubex, 1980). No PRE effects could be measured for residues 7 and 45 in the free and for residues 14, 45, 53 and 86 in the bound forms due to overlap or low signal to noise.

± 18 Hz (15, 20, 24, 35, 41, 43, 44, 51, 67, 69, 88, 90, and 92). The $^1\text{H}^{\text{N}}$ nuclei of the free and bound $^4\text{F1}^5\text{F1}$ species exhibiting the largest PRE

variations between the free and bound forms are shown superimposed upon a ribbon diagram of the $^4\text{F1}^5\text{F1}$ structure in Figures 3a and 3b.

For free $^4\text{F1}^5\text{F1}$ the major PRE effects from the neutral species TEMPOL are for residues H^{N}_{67} and H^{N}_{35} and each is located in a loop exposed to solvent. Assuming that one of the factors promoting TEMPOL- $^4\text{F1}^5\text{F1}$ interactions is the requirement for a hydrophobic environment these residues are located within $\sim 5 \text{ \AA}$ of L73 and L74, and C33, L34 and I41 respectively. The neutral nitroxide species TEMPOL does not affect significantly residues 41, 43, and 88, which are exposed to the solvent, indicating that a hydration shell might prevent a close approach to the protein surface in the corresponding region. For the positively charged nitroxide species 4-amino-TEMPO a large PRE effect is only measured for residue 14, which forms part of a β -strand and, assuming that in this case electrostatic interactions influence the lifetime of the transient interactions, is located within $\sim 5 \text{ \AA}$ of

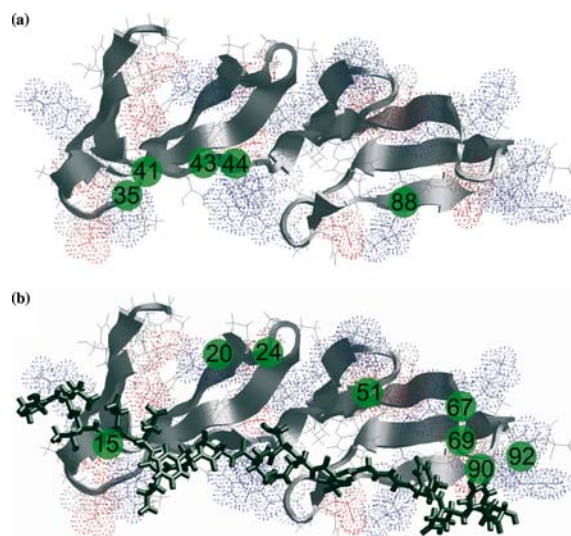


Figure 3. Ribbon diagrams of the $^4\text{F1}^5\text{F1}$ module pair (Williams et al., 1994) (a) free and (b) of a model of $^4\text{F1}^5\text{F1}$ complexed with the peptide D3t. D3t in (b) is shown in green and the acidic and basic side chains of $^4\text{F1}^5\text{F1}$ are highlighted in red and blue respectively by a dotted surface. The $^1\text{H}^{\text{N}}$ nuclei which are more affected by the nitroxide in solution in the free (a) or in the bound (b) forms are highlighted in green. The structure of the complex was derived from an NMR structure of $^4\text{F1}^5\text{F1}$ with manual addition of the D3t peptide using Hyperchem[®] so as to form an additional anti parallel β -strand between the peptide and residues 41–44 and 86–90 of $^4\text{F1}^5\text{F1}$, in the manner predicted previously (Schwarz-Linek et al., 2003).

the negatively charged side chain of residue E17. For the negatively charged species 3-carboxy-PROXYL a larger set of residues exhibit significant transverse PRE effects (24, 25, 43, 44, 88, 41, 67 and 90). All of these are solvent accessible and located within $\sim 5 \text{ \AA}$ of a positively charged side chain (R40 for 41, 43, 44; R83 for 43 and 44; K87 for 88; R90 for 90; K67 for 67; K21 for 24 and 25), which may help to explain why these residues, except 67, are unaffected by the positively charged radical 4-amino-TEMPO. H^{N}_{67} which is affected by both charged radicals is also located near to the negatively charged side chain of D68. Previous studies had demonstrated that TEMPOL, which is uncharged and hydrophobic, might not be able to break through the water shell which surrounds the charged side chains exposed to the solvent (Scarselli et al., 1999, Niccolai et al., 2001). This seems to be the case for H^{N}_{41} , H^{N}_{43} and H^{N}_{88} which are exposed to the solvent, but only the negatively charged nitroxide 3-carboxy-PROXYL is able to influence their transverse relaxation rates significantly. Hence, the current study indicates that charged 3-carboxy-PROXYL and 4-amino-TEMPO (for H^{N}_{14}) might be more able to penetrate the hydration shell, seemingly due to weak electrostatic interactions with the protein (Likhtenshtein et al., 1999).

For free $^4\text{F1}^5\text{F1}$ the $^1\text{H}^{\text{N}}$ nuclei exhibiting a high PRE effect are accessible to the solvent. However accessibility alone is not sufficient to give a significant PRE effect as there are other exposed $^1\text{H}^{\text{N}}$ nuclei which show relatively small effects for at least one of the nitroxide species. This shows and the use of charged radicals suggests that either local electrostatic properties or the presence of a hydration shell might hinder the approach of a nitroxide molecule. Hence, the use of nitroxide species carrying different charges offers the potential for a larger number of accessible surface residues to experience a significant PRE effect.

When the $^4\text{F1}^5\text{F1}$ module pair is complexed to the D3t peptide a significantly reduced PRE effect is found for $^1\text{H}^{\text{N}}_{35}$, $^1\text{H}^{\text{N}}_{41}$, $^1\text{H}^{\text{N}}_{43}$, $^1\text{H}^{\text{N}}_{44}$ and $^1\text{H}^{\text{N}}_{88}$ suggesting these $^1\text{H}^{\text{N}}$ nuclei are no longer accessible to the radical when D3t is bound to $^4\text{F1}^5\text{F1}$. For $^1\text{H}^{\text{N}}_{41}$ a small PRE effect can be observed in the complex, indicating that this residue is still partially accessible to the nitroxide molecules in solution—but the accessibility is

much reduced by binding to D3t. The $^1\text{H}^{\text{N}}$ atoms of residues 15, 20, 24, 51, 67, 69, 90 and 92 exhibit a slightly increased PRE effect ($\sim 20\text{--}100\text{ Hz}$) in the complex compared to the free species suggesting that there are small conformational rearrangements in the protein backbone or side chains leading to some modifications of the protein radical interactions.

The major reduction to the $\Delta R_2(\text{PRE})$ effects caused by the binding of D3t to residues H^{N}_{35} , H^{N}_{41} , H^{N}_{43} , H^{N}_{44} and H^{N}_{88} (Figure 2c) can be compared to the $^1\text{H}^{\text{N}}$ and ^{15}N backbone chemical shift differences caused by complex formation. The binding of D3t peptide leads to many significant backbone $^1\text{H}^{\text{N}}$ and ^{15}N chemical shift perturbations, $\Delta\delta$, and these are shown as a function of residue number in Figures 4a and b respectively. In a system such as this, where the $^4\text{F1}^5\text{F1}$ protein backbone is thought to undergo only limited conformational rearrangement upon ligand binding, the largest backbone protein chemical shift perturbations are usually assumed to identify those residues specifically within or close to the ligand binding site, although the origin of the shift perturbations in this type of system is not well understood. It is interesting to note that for some nuclei there is a correlation between the largest chemical shift changes and the largest changes to the PRE effects upon D3t binding. This applies particularly to residues 41, 43, 44 and 88 (Figures 2c and 3a). The chemical

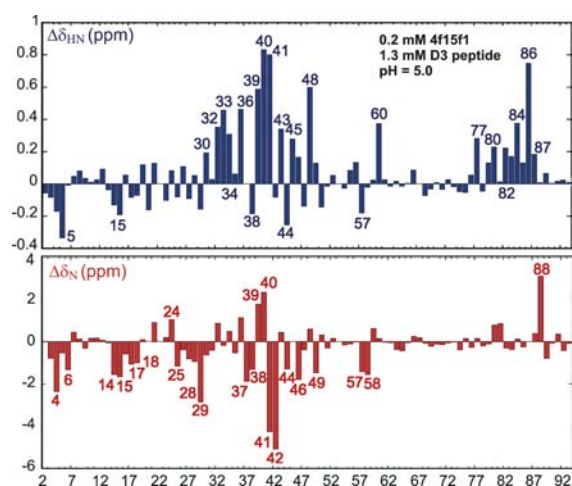


Figure 4. Chemical shift changes for backbone amide protons and nitrogens in $^4\text{F1}^5\text{F1}$ upon binding to D3t (Penkett et al., 2000).

shift differences also show many small differences for residues remote from the binding sites (residues 28–30, 32–35, 48, 57, 58, 60, 77 are close to the binding site but are not directly involved in the binding process).

The change in the transverse relaxation rate of backbone amide protons, $^1\text{H}^{\text{N}}$, has been monitored using three different nitroxide species (3-carboxy-PROXYL, 4-amino-TEMPO and TEMPOL) for the protein $^4\text{F1}^5\text{F1}$ both in the free and bound state.

A small group of residues could be identified whose $^1\text{H}^{\text{N}}$ nuclei were protected from the radicals in the bound state and each of these residues were found to be located close to the known ligand binding site. The bound peptide protects these residues inaccessible to the radicals and they exhibit much reduced PRE effects. Those residues exhibiting the largest changes to the PRE effects upon ligand binding also exhibit significant chemical shift changes. For systems similar to $^4\text{F1}^5\text{F1}$, where the protein is known to undergo only limited conformational changes upon ligand binding, the reductions to the PRE effects caused by the presence of ligand are useful for identifying residues near or in the ligand binding site and these data represent useful starting information for ligand docking programs such as HADDOCK (Dominguez et al., 2003).

The interaction between the fibronectin $^1\text{F1}^2\text{F1}$ module pair and a bacterial fibronectin-binding peptide has been shown to involve the creation of an additional beta strand in a zipper-like mechanism (Schwarz-Linek et al., 2003). The four residues reported here to exhibit the largest reductions to their PRE effects upon the binding of D3t peptide to $^4\text{F1}^5\text{F1}$ (H^{N}_{41} , H^{N}_{43} , H^{N}_{88} and H^{N}_{90}) are located on the same face of the protein and are consistent with this type of zipper model as predicted previously (Schwarz-Linek et al., 2003). The loops containing residues 20, 24, 51, 67 and 69, show enhanced PRE effects upon D3t binding suggesting there are most likely small conformational rearrangements to the protein and changes to the local electrostatic properties.

The use of radical species carrying a different electrostatic charge has been demonstrated to give a more complete picture of the accessible surface than simply using only TEMPOL. Previous studies had demonstrated that TEMPOL

might not be able to break through the water shell which surrounds the charged side chains exposed to the solvent (Scarselli et al., 1999, Niccolai et al., 2001). In the present system, H^N_{41} , H^N_{43} and H^N_{88} , which are all exposed to the solvent, were only affected by the negatively charged nitroxide 3-carboxy-PROXYL. Hence, the current study indicates that charged 3-carboxy-PROXYL and 4-amino-TEMPO (for H^N_{14}) is more able to penetrate the local hydration shell, due to weak electrostatic interactions with the protein (Likhstenshtein et al., 1999).

We have thus demonstrated the significant potential of two charged, stable and water soluble nitroxide species, i.e., 3-carboxy-PROXYL and 4-amino-TEMPO in addition to TEMPOL for probing the surface exposed to solvent. Moreover, the differences between the paramagnetic relaxation enhancements observed for each nitroxide species provides local information about the sign of the local electrostatic potential (negative in the vicinity of residue 14, positive in the vicinity of residues 41, 43 and 88) and the presence or not of a hydration shell (41, 43 and 88 are less affected by TEMPOL).

We used a quantitative measurement of the transverse relaxation rate, which allowed us to use lower concentrations of nitroxide species, allowing more selective effects be observed in the NMR HSQC spectrum.

Acknowledgements

This work was supported by an EMBO fellowship and by the European Union through the research Training Network 'Cross-Correlation' for MD. JB and IDC acknowledge support from BBSRC and the Wellcome Trust respectively. We thank Dr Bernd Schollhorn and Prof. André Rassat (École Normale Supérieure, Paris) for stimulating discussions.

Supplementary material to this paper is available in electronic form at <http://dx.doi.org/10.1007/s10858-004-7912-6>.

References

- Ball, A., Nielsen, R., Gelb, M.H. and Robinson, B.H. (1999) *Proc. Natl. Acad. Sci. USA*, **96**, 6637–6642.
- Barnakov, A., Altenbach, C., Barnakova, L., Hubbell, W.L. and Hazelbauer, G.L. (2002) *Protein Sci.*, **11**, 1472–1481.
- Bhargava, K. and Feix, J.B. (2004) *Biophys. J.*, **86**, 329–336.
- Bodenhausen, G. and Ruben, D.J. (1980) *Chem. Phys. Lett.*, **69**, 185–189.
- Brown, L.J., Sale, K.L., Hills, R., Rouviere, C., Song, L., Zhang, X. and Fajer, P.G. (2002) *Proc. Natl. Acad. Sci. USA*, **99**, 12765–12770.
- Carr, H.Y. and Purcell, E.M. (1954) *Phys. Rev.*, **94**, 630.
- Dominguez, C., Boelens, R. and Bonvin, A.M.J.J. (2003) *J. Am. Chem. Soc.*, **125**, 1731–1737.
- Dwek, R.A. (1973) *NMR in Biochemistry*, Clarendon Press, Oxford, U.K.
- Esposito, G., Lesk, A.M., Molinari, H., Motta, A., Niccolai, N. and Pastore, A. (1992) *J. Mol. Biol.*, **224**, 659–670.
- Gross, A. and Hubbell, W.L. (2002) *Biochemistry*, **41**, 1123–1128.
- Hustedt, E.J. and Beth, A.H. (1999) *Annu. Rev. Biophys. Biomol. Struct.*, **28**, 129–153.
- Likhstenshtein, G.I., Adin, I., Novoselsky, A., Shames, A., Vaisbuch, I. and Glaser, R. (1999) *Biophys. J.*, **77**, 443–453.
- Meiboom, S. and Gill, D. (1958) *Rev. Sci. Instrum.*, **29**, 688–691.
- Molinari, H., Esposito, G., Ragona, L., Pegna, M., Niccolai, N., Brunne, R.M., Lesk, A.M. and Zetta, L. (1997) *Biophys. J.*, **73**, 382–386.
- Niccolai, N., Ciutti, A., Spiga, O., Scarselli, M., Bernini, A., Bracci, L., Di Maro, D., Dalvit, C., Molinari, H., Esposito, G. and Temussi, P.A. (2001) *J. Biol. Chem.*, **276**, 42455–42461.
- Niccolai, N., Rossi, C., Valensin, G., Mascagni, P. and Gibbons, W.A. (1984) *J. Phys. Chem.*, **88**, 5689–5692.
- Pellecchia, M., Sem, D.S. and Wüthrich, K. (2002) *Nat. Rev. Drug Discovery*, **1**, 211–219.
- Penkett, C.J., Dobson, C.M., Smith, L.J., Bright, J.R., Pickford, A.R., Campbell, I.D. and Potts, J.R. (2000) *Biochemistry*, **39**, 2887–2893.
- Prosser, R.S., Luchette, P.A., Westerman, P.W., Rozek, A. and Hancock, R.E.W. (2001) *Biophys. J.*, **80**, 1406–1416.
- Scarselli, M., Bernini, A., Segoni, C., Molinari, H., Esposito, G., Lesk, A.M., Laschi, F., Temussi, P. and Niccolai, N. (1999) *J. Biomol. NMR*, **15**, 125–133.
- Schwarz-Linek, U., Werner, J.M., Pickford, A.R., Gurusiddappa, S., Hwa Kim, J., Pilka, E.S., Briggs, J.A.G., Gough, T.S., Höök, M., Campbell, I.D. and Potts, J.R. (2003) *Nature*, **423**, 177–181.
- Teng, C.L. and Bryant, R.G. (2000) *J. Am. Chem. Soc.*, **122**, 2667–2668.
- Ulmer, T.S., Campbell, I.D. and Boyd, J. (2002) *J. Magn. Reson.*, **157**, 181–189.
- Williams, M.J., Phan, I., Harvey, T.S., Rostagno, A., Gold, L.I., and Campbell, I.D. (1994) *J. Mol. Biol.*, **235**, 1302–1311.